

# Chemistry–A European Journal



Supporting Information

## Proton-Transfer Dynamics of Photoacidic Merocyanines in Aqueous Solution

Christoph Kaiser, Thomas Halbritter, Alexander Heckel, and Josef Wachtveitl\*

# Supporting Information

## Table of contents

Steady-state properties of the Py-BIPS derivative <b>1</b> .....	2
Photo- and ESPT-dynamics of <b>HMCH</b> of compound <b>1</b> .....	3
Steady-state properties of the nitro-BIPS derivatives <b>2</b> and <b>3</b> .....	7
Proton-transfer dynamics of the nitro-BIPS derivative <b>2</b> .....	8
References .....	10

## Steady-state properties of the Py-BIPS derivative 1

The water-soluble compound **1** acts as a highly acidochromic and thus pH-gated photoswitch and shows auspicious performance in a wide pH range from 1 to 12. As the photophysical properties of the compound are quite sophisticated, they're briefly summarised in the following section. A detailed description can be found in our previous report.<sup>[1]</sup> Compound **1** bears a propylsulfonic acid residue, mainly to increase water-solubility which is approximately 10 mM. Between pH 7 and 12 both photoisomers **SP** and **MC** are unprotonated. In the acidic pH regime, compound **1** can be operated as discriminative photochromic systems, due to the existence of multiple protonated states of both isomers. The respective photoswitch systems as well as the absorbance and emission spectra of the isomers at the pH levels of investigation are illustrated in Fig. S1. Despite the structural similarity to the parent Py-BIPS molecule, the photophysical properties of compound **1** are significantly different due to the absence of the methyl group. While the methylated Py-BIPS almost exclusively exists in its energetically favoured spiroopyran form under dark conditions, the merocyanine isomer of compound **1** is strongly stabilised. Hence, the thermal equilibrium between the isomers consists of roughly 50 % of the ring-open conformation at pH 7.4 and 5.5. At these pH values, compound **1** can be operated as a negatively photochromic switch without the necessity for the application of harmful UV light. At pH 1, the content of the ring-open form that can be accumulated is even higher, although the switch appears bistable here and thermal interconversion is halted.

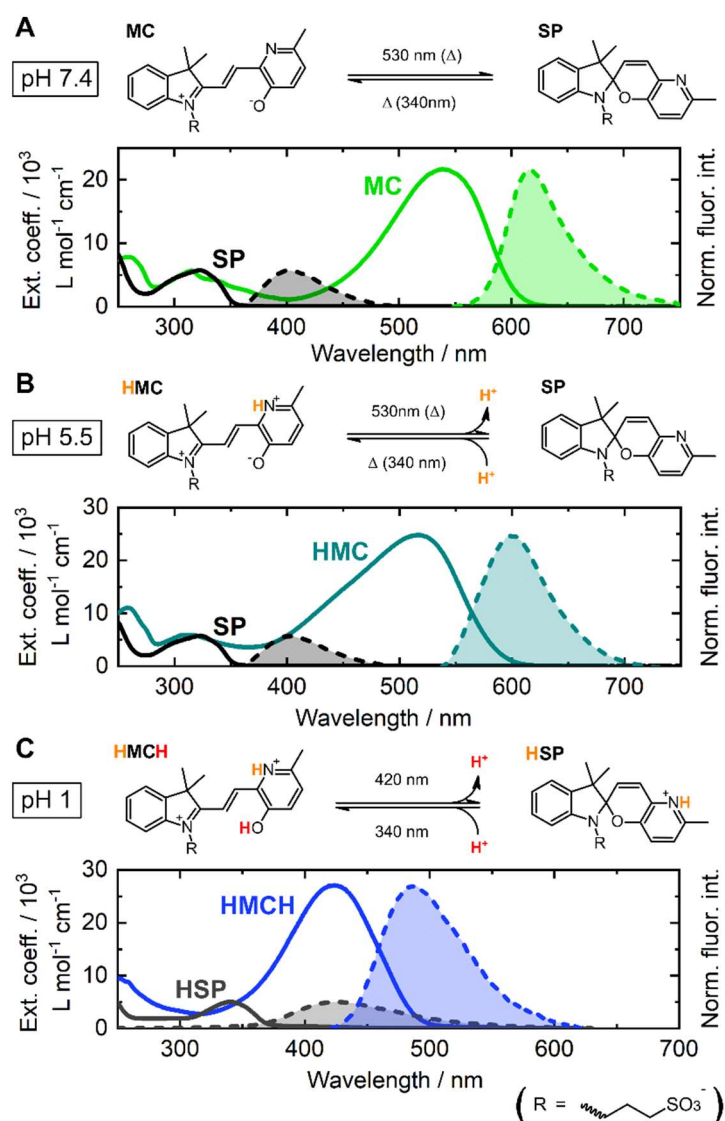


**Figure S1.** Steady-state properties of the Py-BIPS derivative **1** at **A**) pH 7.4, **B**) pH 5.5 and **C**) pH 1 and corresponding absorption and emission spectra of the particular photoisomers and their protonated states.

Upon acidification, the merocyanine isomer is first protonated at its pyridine moiety at pH 5.5 (**HMC**,  $pK_a = 6.8$ ). Protonation is accompanied by a hypsochromic shift of the main absorption band for about 20 nm and of the emission band for 10 nm. The spiropyran isomer is still unprotonated in this pH regime, since the  $pK_a$  value of the respective protonation site is lower in the ring-closed structure (4.8). This implies that upon photoinduced ring-closure, the proton is released and remains dissociated (**SP**) at approximately pH 4.8 and higher until the photoswitch thermally reverts to **HMC**. The solvation of the proton can be detected by the change of the pH value. Therefore, a visible light-driven pH regulation of aqueous solutions in a range roughly between pH 4-7 is feasible with compound **1**.<sup>[1]</sup>

At pH 1, the switch is convertible between the protonated states **HSP** and **HMCH**. Protonation of the ring-closed isomer shifts the absorption band bathochromically for 15 nm, whereas **HMCH** absorbs around 420 nm. This hypsochromic shift of the merocyanine absorbance of about 100 nm is well-known for this protonated species.<sup>[2-4]</sup> The ring-closure is accompanied by the release of the phenolic or rather pyridinolic proton. It could either be transferred to the solvent or to another intramolecular functional group, like the sulfonic acid residue or the indoline nitrogen. The latter can be ruled out, since no spectral changes of the **HSP** band were observed in a pH titration and switching experiment even at very low pH values. This indicates that the  $pK_a$  value of this position must be significantly smaller than 1. The sulfonic acid is also not likely to be protonated due to its high acidity ( $pK_a < 1$ ). However, the flexibility of the propyl chain allows for an approximation of the  $SO_3^-$  group to the phenolic proton. The proton release could therefore be assisted by the vicinity of the sulfonic acid.

### Photo- and ESPT-dynamics of HMCH of compound 1

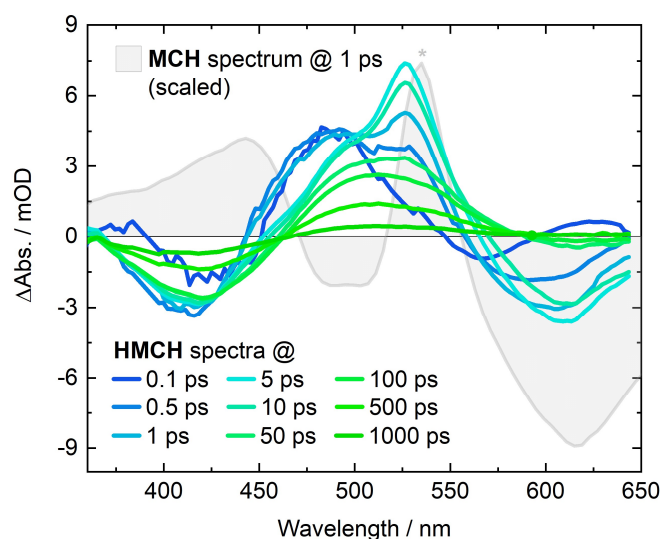


**Figure S2.** Transient absorption difference spectra at fixed delay times of the excited **HMCH** isomer of compound **1**. In addition, the difference spectrum of the excited **MCH** at 1 ps is provided (the asterisk indicates the maximum that has been used for scaling). The positive band around 530 nm (ESA) and the negative around 610 nm (SE) of the **MCH** spectrum are in well agreement with the spectra obtained upon excitation of **HMCH**, which confirms the proton release process.

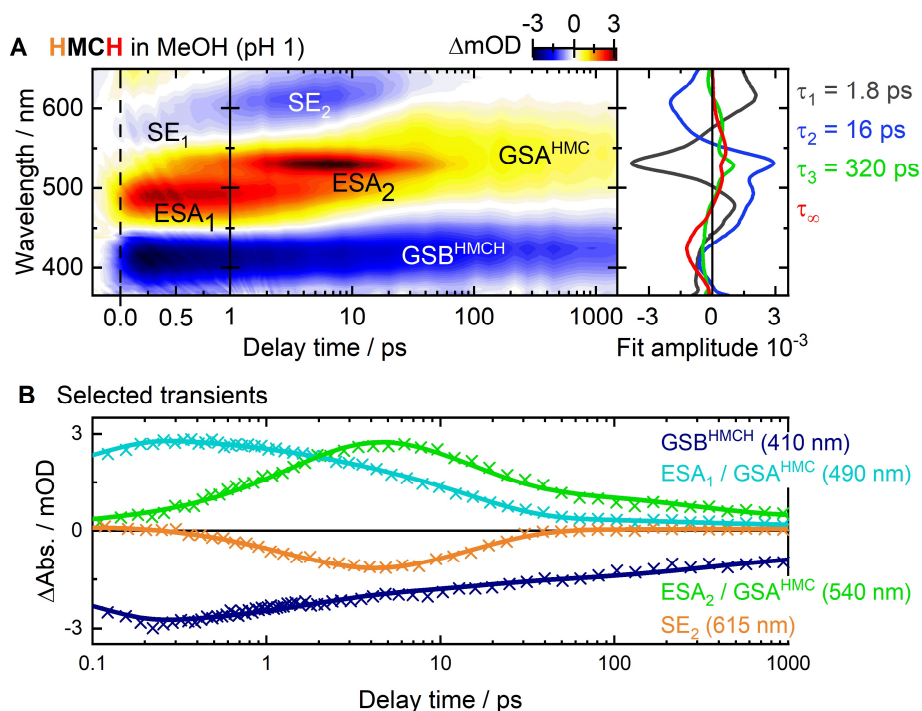


**Figure S3.** TA contour plot of **HMCH** of compound **1** in MeOH (left panel) and corresponding DAS (right panel). **B**) Selected transients showing the time-dependent progression of the particular signals. Data points are represented by symbols (crosses) and the fit from GLA by solid lines.

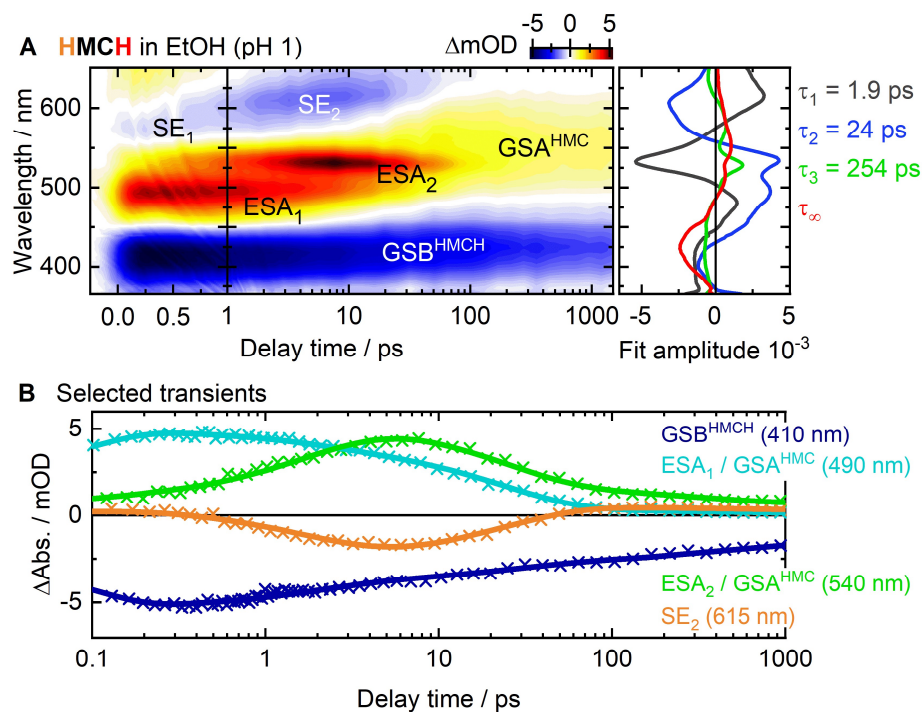


**Figure S4.** TA contour plot of **HMCH** of compound **1** in EtOH (left panel) and corresponding DAS (right panel). **B**) Selected transients showing the time-dependent progression of the particular signals. Data points are represented by symbols (crosses) and the fit from GLA by solid lines.

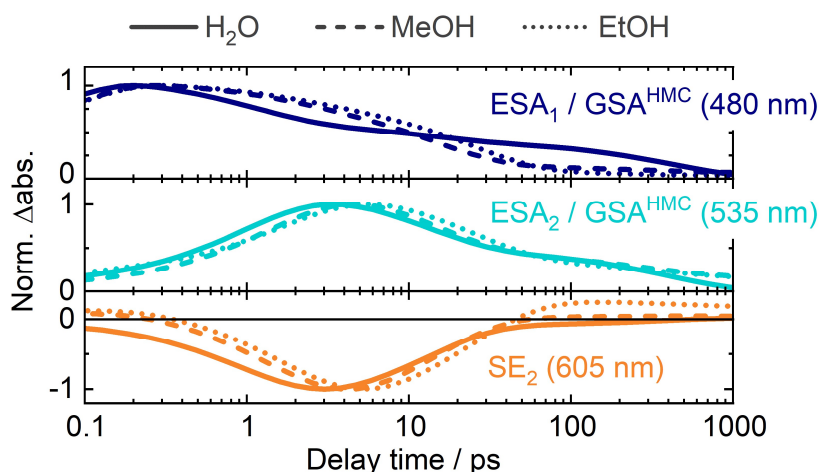


**Figure S5.** Comparison of selected transients of the TA measurements of **HMCH** of compound **1** in H<sub>2</sub>O (solid lines), MeOH (dashed lines) and EtOH (dotted lines). The depicted transients show the fits from the GLA; the datapoints are omitted.

In addition to the data analysis via GLA, lifetime distribution analyses (LDA) were performed on each transient absorption dataset of the excited state PAs in water, MeOH and EtOH using the OPTIMUS software.<sup>[5]</sup> The LDA is a model-free data evaluation method, which is not restricted to a given set of exponential functions and thus not biased by a kinetic scheme. The datasets are fitted with very high number (100) of exponential components and their amplitudes are determined. As a result, the amplitudes are visualised as time- and wavelength-dependent contour plot – the lifetime density map (LDM).<sup>[6]</sup> The obtained LDMs for the three solvents are depicted in Fig. S5 and their reading, is similar as for the DAS. A positive amplitude indicates the decay of a positive signal or the increase of a negative one and vice versa.

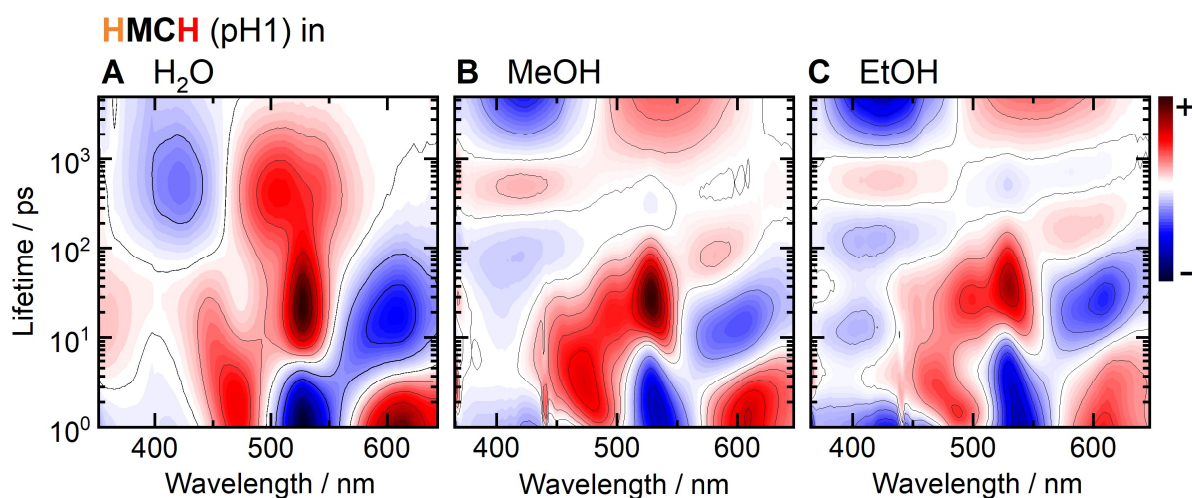


**Figure S6.** Lifetime density maps (LDM) of the proton-release reactions of **HMCH** of compound **1** in **A)** H<sub>2</sub>O, **B)** MeOH and **C)** EtOH. Similar to the reading of DAS, positive amplitudes in the LDM indicate a decay of positive signals or an increase of negative ones. Negative amplitudes correspond to decay of negative signals or increase of positive ones.

Each of the LDMs nicely models the proton transfer dynamics, as discussed in the main text. The positive contributions roughly between 450 nm and 500 nm that last up to about 10 ps capture the decay of ESA<sub>1</sub>. The negative contributions between 500 nm and 550 nm which evolve into positive features account for the formation of ESA<sub>2</sub> and the subsequent decay thereof. Additionally, the positive amplitudes above 580 nm that turn into negative ones model the formation and decay of SE<sub>2</sub> in parallel to ESA<sub>2</sub>. The LDMs clearly reveal, that the formation of ESA<sub>2</sub> is increasingly delayed with decreasing solvent polarity and that it takes longer for the respective signals to decay. At later times, crucial differences to the dynamics in water are predominant in the protic solvents, such as the negative contributions in the range of the GSB

signals around 400 nm on a similar timescale as the decay of  $ESA_2$ . This reflects a transition from the **HMC\*** state directly to the **HMCH** ground state and is therefore assigned to proton-recombination quenching, which was not observed in water. In MeOH, this process occurs on a 50-150 ps timescale, while it takes 90-200 ps in EtOH. Moreover, the LDM corresponding to the EtOH measurement shows an additional negative feature attributed to **HMCH** ground state recovery between 7-20 ps that hints a significant contribution of non-radiative relaxation of **HMCH\***. After roughly 100 ps, the LDM of the measurement in water, exhibits a broad positive feature between 480 nm and 550 nm and a negative one in the range of the GSB. Taken together, these features capture the decay of the **HMC** GSA and a recovery of the **HMCH** ground state and are thus attributed to the reprotonation process within the ground state. In contrast, the formation of the **HMC** ground state is clearly observed in both protic solvents but is not finished after 1.5 ns (see Fig. S3 and S4). The lifetime contributions of the reprotonation as observed in water are thus shifted to later times (<1 ns) in the LDMs of the protic solvents. Instead, there are indications for the excited state reprotonation equilibrium between the initially formed counter ion pair and the fully solvated ions. The positive features around 530 nm evolve into negative ones, which could indicate that the  $ESA_2$  signals slightly increase again after its main decay. Additionally, the negative features around 600 nm that account for the decay of  $SE_2$  turn into positive ones after roughly 50-70 ps.

## Steady-state properties of the nitro-BIPS derivatives **2** and **3**

The photochromic behaviour of both water-soluble nitro-BIPS derivatives **2** and **3** in the neutral pH range is described in our previous publication.<sup>[7]</sup> The attachment of the electron withdrawing nitro groups results in a shift of thermal equilibrium towards the merocyanine form, compared to the methylated py-BIPS compound or the unsubstituted BIPS molecule. Unfortunately, both compounds **2** and **3** are much more vulnerable to hydrolytic decomposition but they are highly stable against photodegradation. In the neutral range, the ring opening reaction can be induced by UV irradiation around 350 nm, whereas the ring closing reaction is initiated by vis light. The **MC** form of nitro-BIPS **2** exhibits a main absorption band around 510 nm and that of dinitro-BIPS **3** is centred around 495 nm (Fig. S7). Both show fluorescence emission, the **MC** isomer of **2** around 640 nm and that of **3** around 600 nm.

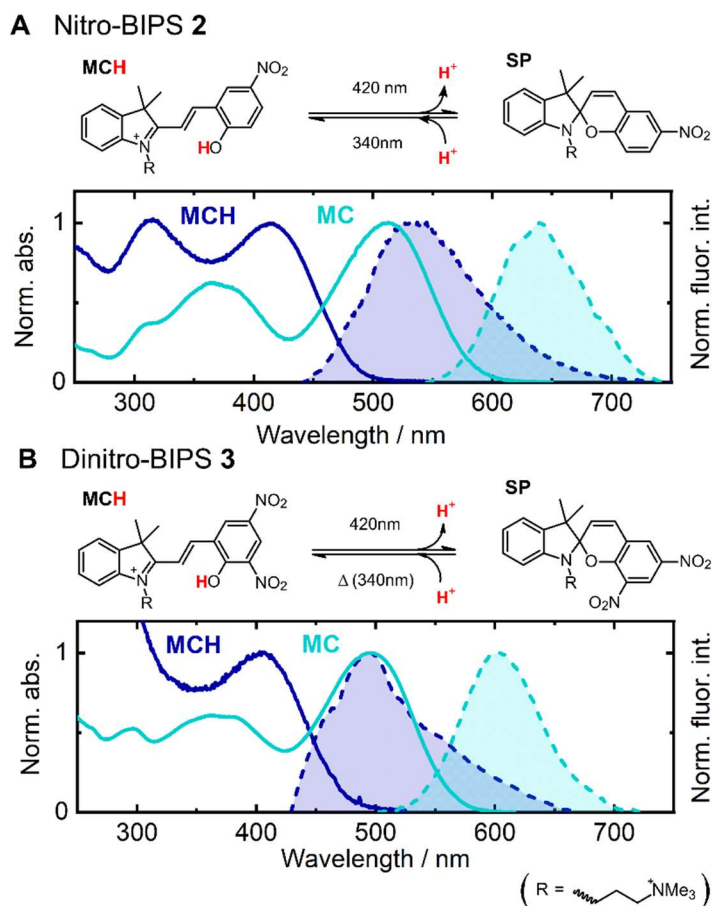


**Figure S7.** Photoisomerisation between **MCH** and **SP** of **A**) nitro-BIPS **2** and **B**) dinitro-BIPS **3** at pH 1. The graphs show the steady-state absorption (solid lines) and emission spectra (dashed lines) of the unprotonated **MC** (dark blue) and the protonated **MCH** (light cyan).

Upon acidification, the phenolate oxygen is protonated which gives **MCH** with a  $pK_a$  value of 3.7 for **2** and 3.9 for **3**. The main absorption bands are shifted hypsochromically for about 90 nm, compared to **MC**. After dissolving compound **2** in aqueous solution at pH 1 or lower, an **SPH** sample is obtained, where the indole nitrogen is protonated.<sup>[2]</sup> The open-ring **MCH** form can be accumulated by heating the sample or by illumination with 340 nm light. Yet, the sample does not revert to the closed isomer thermally. As to compound **3**, a pure **MCH** sample is directly obtained, since the open ring conformation is thermodynamically favoured. Fluorescence emission of **MCH** is only observed at pH values below 0 for both derivatives and the emission is very weak. At higher pH values, the emission bands of the **MC**

forms are detected. This implies that upon excitation of **MCH**, fluorescence emission occurs from the **MC\*** state after proton release within the excited state. The **MCH** isomer of compound **2** fluoresces at 530 nm and that of compound **3** around 495 nm, where the absorption band of the unprotonated **MC** is located.

### Proton-transfer dynamics of the nitro-BIPS derivative **2**

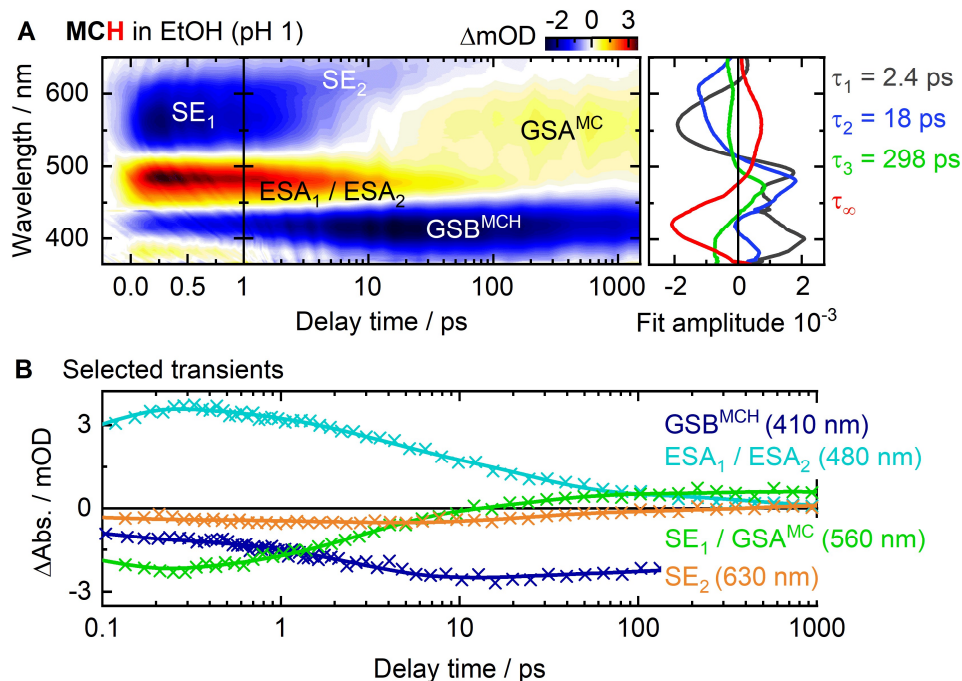


**Figure S8.** TA contour plot of **MCH** of compound **2** in EtOH (left panel) and corresponding DAS (right panel). **B**) Selected transients showing the time-dependent progression of the particular signals. Data points are represented by symbols (crosses) and the fit from GLA by solid lines.

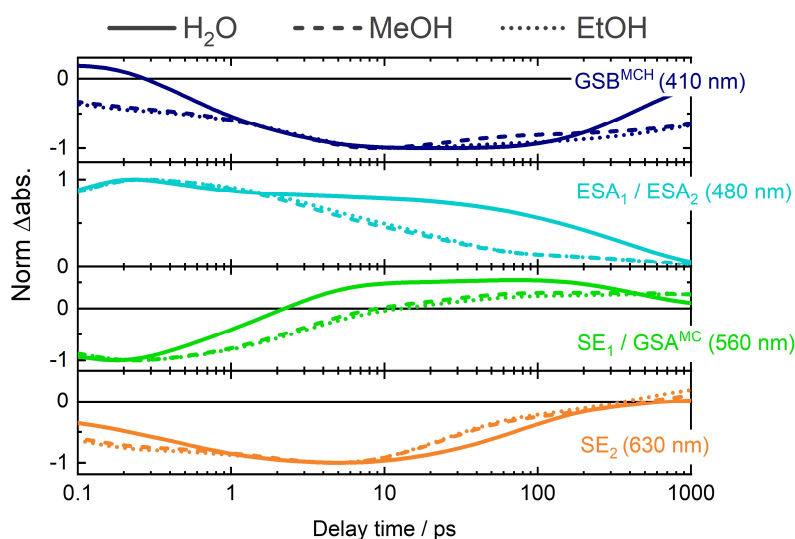


**Figure S9.** Comparison of selected transients of the TA measurements of **MCH** of compound **2** in H<sub>2</sub>O (solid lines), MeOH (dashed lines) and EtOH (dotted lines). The depicted transients show the fits from the GLA; the datapoints are omitted.

The transient absorption datasets of **MCH** of compound **2** in water and both protic solvents were also subjected to LDA. The obtained LDMs are depicted in Fig. S9. The negative contributions roughly between 500 nm and 600 nm that last up to about 10 - 20 ps capture the decay of  $SE_1$  and thus the decay of the **MCH\*** state. At later times these features evolve into red-shifted negative lifetime contributions above 600 nm which capture the subsequent decay of  $SE_2$ . Regarding the protic solvents, the respective lifetime contributions are drastically smaller than in water. In the range of the  $ESA_1$  /  $ESA_2$  signals from 450 nm to 500 nm, the LDM of the water measurement reveals the initial decay of the positive signal and the negative amplitude around 10 ps models the slight increase, which is another evidence for the superposition of the two superimposed ESA signals in the TA map (Fig. 4A). This is not monitored in the LDMs of the protic solvents but a continuous positive feature.

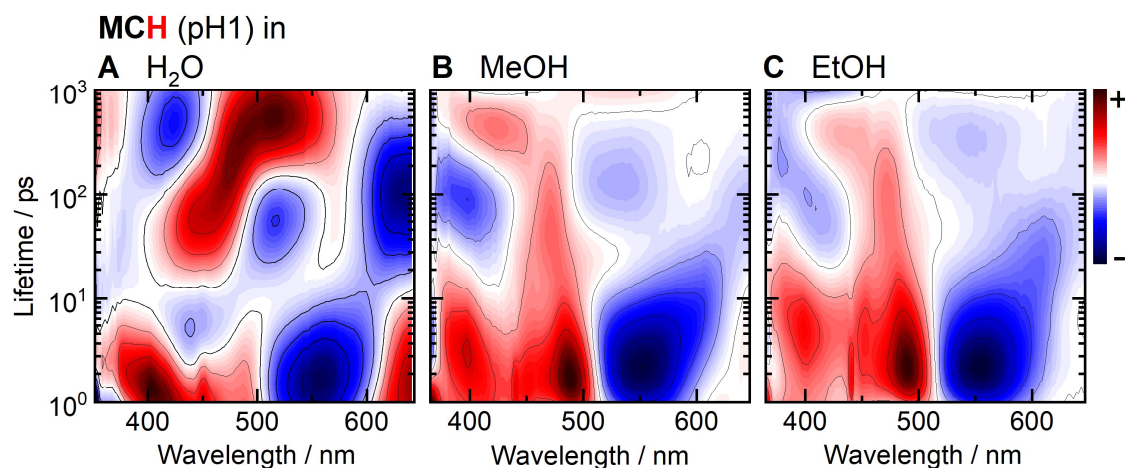


**Figure S10.** Lifetime density maps (LDM) of the proton-release reactions of **MCH** of compound **2** in **A)**  $H_2O$ , **B)** MeOH and **C)** EtOH. Similar to the reading of DAS, positive amplitudes in the LDM indicate a decay of positive signals or an increase of negative ones. Negative amplitudes correspond to decay of negative signals or increase of positive ones.

Up to roughly 10 ps, the intense positive contributions are assigned to the decay of **MCH\*** and thus to the proton release. After 10 ps a slight blueshift of those positive features can be noted, which then prevail up to 300 - 400 ps. These features represent the decay of the conjugate base **MC\*** whose lifetime is elongated in protic solvents. The decay thereof is accompanied by the formation of the **MC** ground state, which is captured by the negative contributions between 500 nm and 575 nm at roughly 100 - 200 ps (MeOH) and 300 - 400 ps (EtOH). In the GLA, lifetimes of roughly 300 ps were determined on both protic solvents but the LDMs reveal that this process actually occurs at later times in EtOH. The fact the GSA signal is already observable earlier in the corresponding TA maps supposedly arises from a faster decay of a discriminable merocyanine conformer. Through GLA, lifetimes of 17 ps (MeOH) and 18 ps (EtOH) with similar amplitudes were determined. Around this time range, the LDMs show a hypsochromic shift of the positive contributions from 490 nm to 475 nm, which confirms the assignment of different isomers with distinguishable ESA properties decaying on different timescales. As this positive lifetime contribution appears as a continuous feature in the LDMs, the shift could account for an excited state isomerisation from one conformer into the other. At late delay times (< 1 ns), the LDMs reflect the residual positive **MC** ground state absorption signal as well as the remaining GSB of **MCH**.

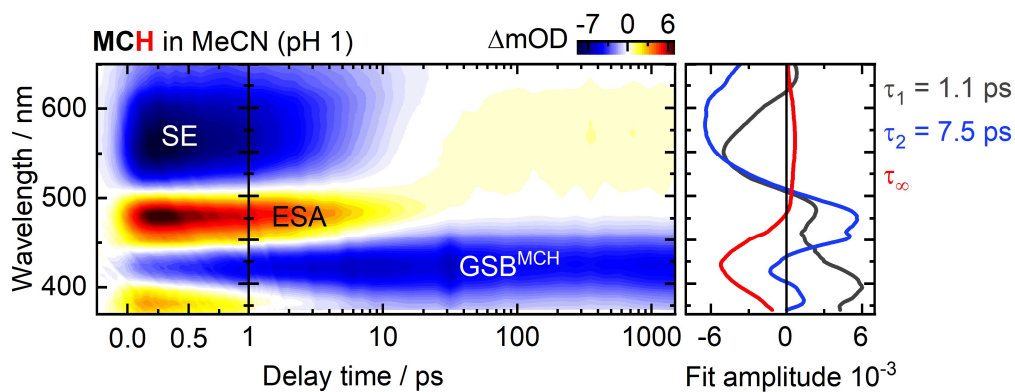


**Figure S11.** TA contour plot of **MCH** of compound **2** in MeCN (left panel) and corresponding DAS (right panel).

## References

- [1] T. Halbritter, C. Kaiser, J. Wachtveitl, A. Heckel, *J. Org. Chem.* **2017**, *82*, 8040–8047.
- [2] M. Hammarson, J. R. Nilsson, S. Li, T. Beke-Somfai, J. Andréasson, *J. Phys. Chem. B* **2013**, *117*, 13561–13571.
- [3] V. K. Johns, Z. Wang, X. Li, Y. Liao, *J. Phys. Chem. A* **2013**, *117*, 13101–13104.
- [4] Z. Shi, P. Peng, D. Strohecker, Y. Liao, *J. Am. Chem. Soc.* **2011**, *133*, 14699–14703.
- [5] C. Slavov, H. Hartmann, J. Wachtveitl, *Anal. Chem.* **2015**, *87*, 2328–2336.
- [6] R. Croce, M. G. Müller, R. Bassi, A. R. Holzwarth, *Biophys. J.* **2001**, *80*, 901–915.
- [7] C. Kaiser, T. Halbritter, A. Heckel, J. Wachtveitl, *ChemistrySelect* **2017**, *2*, 4111–4123.